IEEE Access
Multidisciplinary | Rapid Review | Open Access Journal

Received December 27, 2020, accepted January 4, 2021, date of publication January 18, 2021, date of current version January 22, 2021.

Digital Object Identifier 10.1109/ACCESS.2021.3051933

Packet-Level Index Modulation for LoRaWAN

KOICHI ADACHI[1], (Senior Member, IEEE), KOHEI TSURUMI[1], AOTO KABURAKI[1], (Graduate Student Member, IEEE), OSAMU TAKYU[2], (Member, IEEE), MAI OHTA[3], (Member, IEEE), AND TAKEO FUJII[1], (Member, IEEE)

[1]Advanced Wireless and Communication Research Center, The University of Electro-Communications, Tokyo 182-8585, Japan
[2]Department of Electrical and Computer Engineering, Shinshu University, Nagano 380-8553, Japan
[3]Department of Electronics Engineering and Computer Science, Fukuoka University, Fukuoka 814-0180, Japan

Corresponding author: Koichi Adachi (adachi@awcc.uec.ac.jp)

This research work was supported by MIC/SCOPE under Grant 205004001.

ABSTRACT The long range wide area network (LoRaWAN) is one of the enabling technologies for low power wide area (LPWA) networks. In LoRaWAN, a node transmits its packet to a gateway (GW) in an autonomous and decentralized manner. The quantity of data that can be transmitted by each node is limited by the duty cycle (DC). Furthermore, it is not easy for the nodes to perform sophisticated techniques for increasing the data quantity due to their limited functionality, especially when the nodes are battery-powered. If the network size increases, packet collision may occur more frequently. Since the packet transmission drains the LoRaWAN nodes' battery, the packet collision results in a waste of limited power. Thus, it is necessary to develop a simple but effective transmission strategy that efficiently utilizes limited battery at each LoRaWAN node. This study proposes packet-level index modulation (PLIM), which is suitable for such LPWA networks. PLIM takes advantage of the sparse data packet transmission in time and the selection of a frequency channel among multiple ones by each node. A time slot and frequency channel combination is selected, i.e., the index, to increase the data quantity. For long-range communication, it is necessary to use a higher spreading factor (SF) in LoRaWAN, which results in a lower data rate due to the DC. The proposed PLIM can compensate for such data rate loss by taking advantage of the sparse transmission in time. Numerical evaluation elucidates that the proposed PLIM can increase the data quantity of LoRaWAN system without requiring any modification in the specification. When the SF is 10, the proposed PLIM can increase the data quantity up to 32.5%, compared to the conventional LoRaWAN system.

INDEX TERMS LPWA, LoRaWAN, index modulation.

I. INTRODUCTION

With the emerge of the Internet-of-Things (IoT), the low power wide area network (LPWAN) is becoming a crucial wireless network structure. The main application of LPWAN includes sensor networks that collect information from each sensor node in a fixed time interval. The long range wide area network (LoRaWAN), which is a type of LPWAN, adopts chirp spread spectrum (CSS) modulation as the physical layer technology [1]. CSS modulation enables long-range and low-power communication. *The spreading factor (SF)*, which determines the LoRaWAN transmission rate [1], indicates the number of bits that can be transmitted by a CSS-modulated symbol. In the LoRaWAN specification, six values (7, 8, $\cdots$, 12) are determined for the SF. Different SFs provide different characteristics; on selecting a higher SF, the communication range can be increased due to its higher resiliency against noise and interference. However, the time length of a CSS-modulated symbol increases, and the data that can be conveyed in a packet reduces [2].

In LoRaWAN, each node transmits its CSS-modulated packet in an autonomous and decentralized manner by pseudorandomly selecting one of the preassigned frequency channels. When multiple nodes transmit data packets simultaneously using the same frequency channel, packet collision occurs. Interference is caused by the same as well as different SF signals due to pseudorthogonality [3]. Thus, packet collision occurs more frequently as the number of LoRaWAN nodes increase within the network, limiting the scalability of LoRaWAN. Numerous studies have been undertaken to the increase the capacity of LoRaWAN. Another performance limitation is caused by the duty cycle (DC), which

The associate editor coordinating the review of this manuscript and approving it for publication was Noor Zaman.

determines the duration for which each node can transmit a data packet over air. Thus, each LoRaWAN node must stop packet transmission immediately after completing its transmission in order to satisfy the DC requirement. In ''The Things Network public community network'', which is one of the largest LoRaWAN networks, a fair access policy has been introduced [4]. This policy limits the data that can be sent by each LoRaWAN node more stringently, i.e., an average of 30 [s] uplink time on air, per 24 h. Furthermore, it is not easy for the node to adopt sophisticated strategies for increasing the data quantity due to its limited functionality and battery capacity.

Thus, it is necessary to develop a simple but effective transmission strategy for increasing the transmission rate without additional battery consumption at each LoRaWAN node, while avoiding frequent packet collisions.

This study proposes *packet-level index modulation (PLIM)*, suitable for LoRaWAN. *PLIM takes advantage of the DC that limits the performance of LoRaWAN*. From a specific node, the consecutive packet transmission interval is considerably longer than the packet length. The transmission interval is divided into a number of time slots; the combination of a time slot and frequency channel is called *index*. After generating data, the node splits it into two parts: the first part is transmitted by the conventional packet and the second part is transmitted by selecting the index. PLIM has two advantages: (i) A node can increase the transmission rate and (ii) the time length of each packet can be reduced. Furthermore, extensive computer simulation evaluation is conducted to establish the effectiveness of the proposed PLIM, based on Japanese parameter configuration AS923. The simulation results demonstrate that the proposed PLIM can increase the number of bits conveyed by a data packet by up to approximately 32.5%, when the SF is set to 10.

The remainder of this paper is organized as follows. In Section II, we briefly introduce the related works. In Section III, the system model of a conventional LoRaWAN system is described. Section IV details the concept of the proposed PLIM. The theoretical performance limits of the proposed PLIM and the computer simulation results are presented in Section V. Section VI concludes the paper.

II. RELATED WORK

A. LoRaWAN NETWORK

There are three main approaches to improve the transmission performance of LoRaWAN: (i) Improving the interference resiliency [6]–[8], (ii) reducing the number of packet collisions through resource management [9]–[13], and (iii) increasing the number of bits conveyed by a CSS symbol [14]. In [6], an SF and coding rate allocation algorithm have been proposed for maximizing the throughput of each SF tier comprising nodes using the same SF. [7] optimizes SF allocation in order to maximize the packet success probability (PSP) and achieve maximum connectivity. In [8], SF assignment strategy has been proposed by considering Time-on-Air (ToA) and capture effect at the GW. In [9], the carrier sense multiple access with collision avoidance (CSMA/CA) mechanism is applied to improve the performance of LoRaWAN. Although (CSMA/CA) has been introduced in LoRaWAN for avoiding simultaneous transmission [10], the carrier sense (CS) mechanism increases the node energy consumption. Reinforcement learning based on frequency channel allocation has been proposed to avoid packet collision [11]. However, these approaches only try to achieve transmission performance where there is no packet collision. Thus, the performance continues to be limited by the DC. In [12], multihop communication technology has been introduced to improve the packet delivery rate (PDR). A low overhead scheduling strategy has been proposed to avoid packet collision through out-of-band synchronization among LoRaWAN nodes in [13]. The authors in [14] proposes interleaved chirp spreading (ICS) LoRa-based modulation. The interleaved version of the CSS symbol can add an extra bit. Thus, ICS has been shown to reduce packet collision by creating new multidimensional space.

B. INDEX MODULATION (IM) AND ITS APPLICATION IN THE MULTIPLE ACCESS SCHEME

Index modulation (IM) can convey additional information by activating a subset of indices on top of the classical physical layer modulation schemes. This additional information is modulated in the spatial [15], frequency [16], and space-time domains. For example, in orthogonal frequency division multiplexing (OFDM) with IM, a subset of the frequency domain subcarriers are activated in each OFDM symbol to convey additional bits. OFDM-IM can improve the transmission performance in a low-rate scenario [18]. [19] proposes index modulation orthogonal frequency division multiplexing access (IM-OFDMA), where some of the information bits are modulated conventionally and the index of the active subcarriers transmits the remaining information bits. In [20], IM on single carrier-frequency division multiple access (SC-FDMA) uplink transmission has been proposed for cellular IoT and machine-to-machine (M2M) networks. [21] implements joint code-frequency-index modulation (CFIM) by considering code and frequency domains for IM. CFIM has been shown to enhance the spectral and energy efficiencies, while maintaining the reliability significantly. In [22], the concept of IM in the context of broadband SC systems and symbol allocation, which is capable of reducing the effect of interchannel correlation, has been proposed.

In [17], the index modulation-multiple access (IMMA) has been proposed. In IMMA, each uplink node selects one of the time slots based on the data that the node attempts to send. As multiple nodes may share the same time slot, interference cancellation is performed on the receiver side.

The PLIM proposed in this study differs from the other IM schemes; it does not require synchronization among the LoRaWAN nodes for specifying the time slots. Moreover, PLIM utilizes both time and frequency as indices. As IM is performed at the packet level in PLIM, the receiver can easily

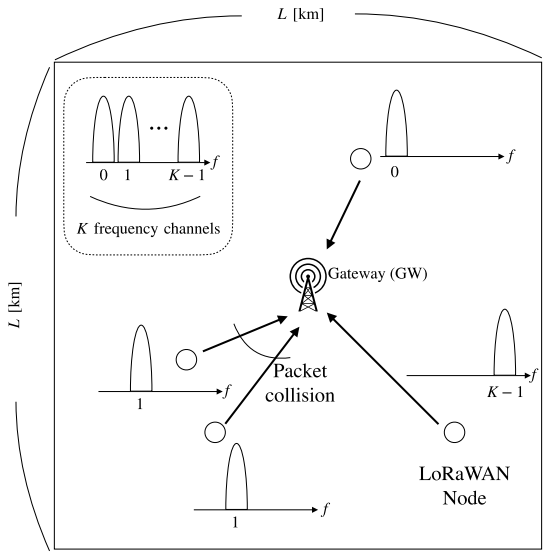

FIGURE 1. Network model.

identify the LoRaWAN nodes. Thus, CSS data modulation and IM can be designed separately.

III. SYSTEM MODEL

A. NETWORK MODEL

This study considers a LoRaWAN network comprising one gateway (GW) and M LoRaWAN nodes (set $\mathcal{M} = \{0, 1, \cdots, m, \cdots, M-1\}$). The GW is located at the center of an $L \times L$ [km^2] communication area and receives data packets from the LoRaWAN nodes, which are randomly and uniformly distributed in the area. In total, K orthogonal frequency channels (set $\mathcal{K}$) are assumed to be available in the system. Each LoRaWAN node periodically transmits data packets restricted by its DC. The CS mechanism is not considered due to the limited capability of the LoRaWAN nodes. The packet generation interval of LoRaWAN node $m \in \mathcal{M}$ is $T_{\text{frame},m}$ [s]. Random offset $T_{\text{os},m} \sim \mathcal{U}\left[0, T_{\text{frame},m}\right]$ is assigned to LoRaWAN node m. This node transmits data packets with SF $S_m \in \mathcal{S} = \{7, 8, 9, 10, 11, 12\}$ in frequency channel $k_m \in \mathcal{K}$, which is randomly selected from the available frequency channels $\mathcal{K}$. Each SF has its own data rate, signal-to-noise power ratio (SNR) threshold Γ_{SNR,S_m}, and signal-to-interference power ratio (SIR) threshold Γ_{SIR,S_m}, as shown in Table 2. Without loss of generality, we consider the operation of LoRaWAN node $m \in \mathcal{M}$.

B. PACKET STRUCTURE

Assuming bandwidth W [Hz] and SF $S_m \in \mathcal{S}$, the CSS-modulated-symbol length $T_{\text{sym},m}(S_m)$ [s] is expressed as [1]

$$T_{\text{sym},m}(S_m) = 2^{S_m}/W. \tag{1}$$

As S_m increases, the transmitted signal becomes more robust against noise, i.e., the SNR threshold $\Gamma_{\text{SNR},m}$ reduces, as shown in Table 2. Thus, nodes located far from the GW need to use higher SF for packet transmission. However, this is achieved at the expense of the data rate. Eq. (1) indicates that the CSS-modulated-symbol length $T_{\text{sym},m}(S_m)$ becomes double and the number of bits per CSS symbol is increased by one, when S_m increases by one. Thus, for the given time length used for packet transmission, the number of bits that each LoRaWAN node can transmit decreases.

Each packet transmitted from LoRaWAN node m comprises multiple CSS-modulated symbols including a preamble, overhead (size: B_{oh} [bit]), and payload (size: B_{pl} [bit]). The maximum payload size $B_{\text{pl}}^{\max}(S_m)$ is specified in the standardization. The number of CSS-modulated symbols within one packet is expressed as [1]

$$N_{\text{sym},m}(S_m) = N_{\text{p}} + \left\lceil \frac{\left(B_{\text{oh}} + B_{\text{pl}}\right)/R}{S_m} \right\rceil, \tag{2}$$

where $\lceil x \rceil$ is the ceiling function of x, N_{p} is the number of CSS symbols in the preamble and overhead, and $R \in \{4/5, 4/6, 4/7, 4/8\}$ is the coding rate. Thus, packet length $T_{\text{pckt},m}$ [s] is expressed as

$$T_{\text{pckt},m}(S_m) = T_{\text{sym},m}(S_m) \times N_{\text{sym},m}(S_m). \tag{3}$$

LoRaWAN node m transmits *only one packet* during $T_{\text{frame},m}$ [s] in order to satisfy the DC requirements (Fig. 2 (a)), i.e., $T_{\text{pckt},m}/T_{\text{frame},m} \leq Q_{\text{DC}}$.

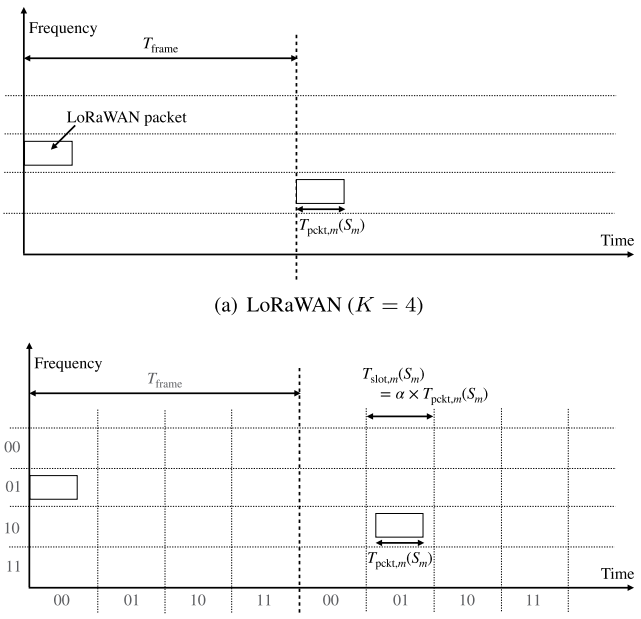

(a) LoRaWAN ($K = 4$)

(b) LoRaWAN with PLIM ($K = 4$ and $Q(S_m, \alpha) = 4$)

FIGURE 2. Packet transmission example.

The data quantity $B_{\text{conv},m}$ [bit] transmitted by one packet in the conventional LoRaWAN is given by

$$B_{\text{conv},m} = B_{\text{pl}}. \tag{4}$$

IV. PACKET-LEVEL INDEX MODULATION (PLIM) IN LoRaWAN

In this section, we describe the principle of the proposed PLIM and its operation.

A. PLIM PRINCIPLE

Each LoRaWAN node periodically transmits data packets that are sparse in time due to the DC restriction and the limited battery capability of the LoRaWAN nodes. The proposed PLIM takes advantage of this characteristic of LoRaWAN to increase the quantity of data that each data packet can convey. In PLIM, the combination of the time slot and frequency channel in which the LoRaWAN node transmits its packet, represents the additional data (Fig. 2 (b)).

The nodes are not necessarily synchronized with each other in PLIM, as shown in Fig. 3, which is different from IMMA that requires the nodes to be synchronized [17]. LoRaWAN node m informs the GW of its starting time for the first frame, i.e., $T_{m,0}$.[1] As packet transmission from each node is periodic, the GW can track the starting time of the subsequent frames. Stringent clock synchronization may not be possible in the simple and cheap LoRaWAN node; hence, clock jitter may impact the PLIM transmission performance because the LoRaWAN node may not be able to transmit a packet in its intended time slot. For synchronization among nodes, the technique proposed in [23] can be adopted.

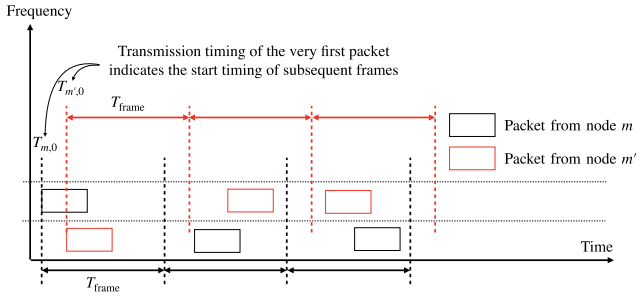

FIGURE 3. Example of asynchronous transmission from two LoRaWAN nodes.

Once the GW knows transmission interval $T_{\text{frame},m}$ [s] of LoRaWAN node m, it can determine the time slot for LoRaWAN node m. The proposed PLIM can offer additional benefits. Suppose multiple nodes transmit data packets simultaneously on the same frequency channel, it is highly probable that they may collide with each other in the subsequent transmissions due to periodic data transmission. On the other hand, in PLIM, each node information quasirandomly determines the time slot and frequency channel. Thus, the collision probability can be lowered.

B. TIME SLOT SETUP

The time slot length $T_{\text{slot},m}(S_m)$ [s] is set as follows:

$$T_{\text{slot},m}(S_m) = \alpha \times T_{\text{pckt},m}(S_m), \tag{5}$$

where $T_{\text{pckt},m}(S_m)$ is the packet length given by Eq. (3), and $\alpha \geq 0$ is the *time slot scaling factor* introduced in order to absorb the clock jitter due to the LoRaWAN node capability.

[1]For example, each LoRaWAN node transmits a packet using $q_m = 0$ at a fixed interval such that the GW can understand the starting time of the first frame.

With $T_{\text{slot},m}(S_m)$, the number of time slots within a frame $Q(S_m, \alpha)$ is given by

$$Q(S_m, \alpha) = \left\lfloor \frac{T_{\text{frame},m}}{T_{\text{slot},m}(S_m)} \right\rfloor = \left\lfloor \frac{T_{\text{frame},m}}{\alpha \times T_{\text{pckt},m}(S_m)} \right\rfloor, \tag{6}$$

where $\lfloor x \rfloor$ is the floor function of x.

Eq. (6) indicates that a smaller α results in a larger number of time slots $Q(S_m, \alpha)$; hence, the additional number of data bits conveyed by the index can increase. However, a smaller α requires more stringent time synchronization between each LoRaWAN node and the GW. The impact of α on the performance improvement obtained using the proposed PLIM is evaluated through computer simulation. The impact of synchronization of the LoRaWAN node on the selection of α is intended for future study.

C. INDEX SETUP

When the number of frequency channels is K and the number of time slots is $Q(S_m, \alpha)$, the number of time slot and frequency channel combinations becomes $K \times Q(S_m, \alpha)$. The index represents the time slot and frequency channel combination selected from $\mathcal{K} \times \mathcal{Q}(S_m, \alpha)$, where $\times$ denotes the Cartesian product. Let $\mathcal{F}_m : \mathcal{B}_{\text{plim},m}(K, Q(S_m, \alpha)) \rightarrow \mathcal{K} \times \mathcal{Q}(S_m, \alpha)$ be an arbitrary mapping function from $B_{plim,m}(K, Q(S_m, \alpha))$ [bit] to index (k_m, q_m).[2] Thus, selecting index $(k_m, q_m) \in \mathcal{K} \times \mathcal{Q}(S_m, \alpha)$ provides additional number of data bits that can be conveyed by one packet, as follows:

$$B_{\text{plim},m}(K, Q(S_m, \alpha)) = \left\lfloor \log_2(K \times Q(S_m, \alpha)) \right\rfloor. \tag{7}$$

Using LoRaWAN with PLIM, the data that can be conveyed by a data packet is

$$\begin{aligned} B_{\text{prop},m} &= B_{\text{pl}} + B_{\text{plim},m}(K, Q(S_m, \alpha)) \\ &= B_{\text{pl}} + \left\lfloor \log_2(K \times Q(S_m, \alpha)) \right\rfloor, \end{aligned} \tag{8}$$

Note that the mapping between the index, and the frequency channel and time slot combination are arbitrarily designed.

D. TRANSMITTER OPERATION

After LoRaWAN node m generates information bit sequence $\mathbf{B}_m \in \{0, 1\}^{B_{\text{prop},m} \times 1}$ [bit] to be transmitted to the GW, it splits the sequence into two $\mathbf{B}_{\text{pl},m} \in \{0, 1\}^{B_{\text{pl}} \times 1}$ [bit] and $\mathbf{B}_{\text{plim},m} \in \{0, 1\}^{\lfloor \log_2(K \times Q(S_m, \alpha)) \rfloor \times 1}$ [bit]; sequence $\mathbf{B}_{\text{pl},m}$ is transmitted through conventional CSS modulation, whereas sequence $\mathbf{B}_{\text{plim},m}$ is transmitted through the index.

First, LoRaWAN node m generates a data packet based on $\mathbf{B}_{\text{pl},m}$ [bit]. The generated data packet is then transmitted on frequency channel k_m $\mathcal{K}$ at time slot $q_m \in \mathcal{Q}(S_m, \alpha)$, which are determined as follows:

$$(k_m, q_m) = \mathcal{F}_m(\mathbf{B}_{\text{plim},m}). \tag{9}$$

[2]The design of the mapping function $\mathcal{F}_m$ is beyond the scope of this study.

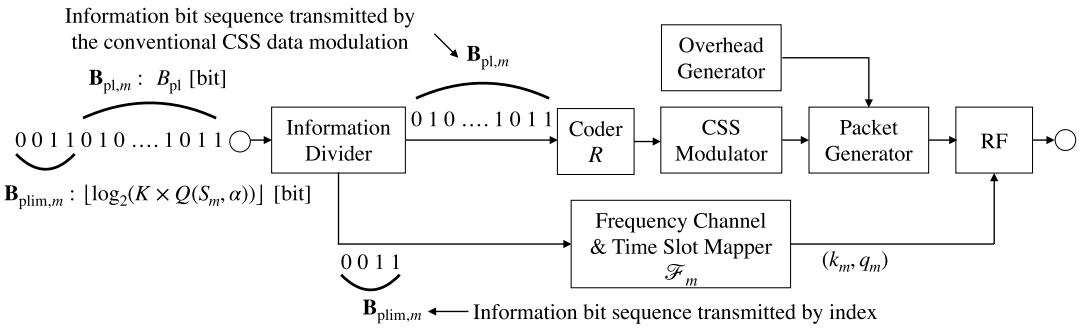

(a) Transmitter structure for LoRaWAN node m

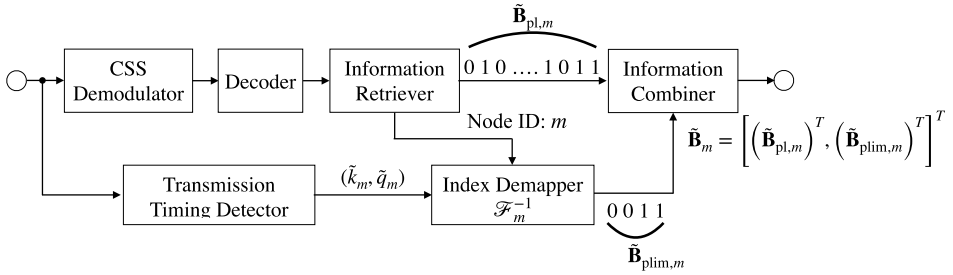

(b) Receiver

FIGURE 4. Transmitter and receiver structure of the LoRaWAN with PLIM.

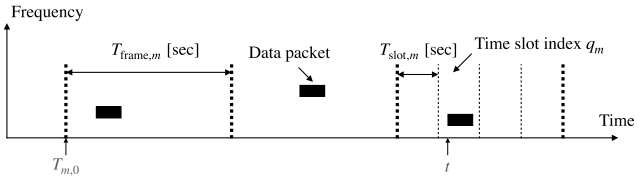

FIGURE 5. Time slot determination at the GW.

E. RECEIVER OPERATION

On receiving a packet from a LoRaWAN node, the GW demodulates the data packet to obtain the overhead and payload $\tilde{\mathbf{B}}_{\mathrm{pl},m}$. The node identification (ID) in the data packet enables the GW to retrieve the starting time of the LoRaWAN node. Suppose that a data packet is transmitted from LoRaWAN node m. Let t [s] be the time at which the GW receives the packet. Then, the GW determines time slot index q_m by solving the following equation (Fig. 5):

$$\tilde{q}_m = \left\lfloor \frac{\mathrm{mod}\left(t - T_{m,0}, T_{\mathrm{frame},m}\right)}{T_{\mathrm{slot},m}(S_m)} \right\rfloor, \tag{10}$$

where mod (,) denotes modulo operation. As the GW can decipher the frequency channel $\tilde{k}_m \in \mathcal{K}$, it can obtain the information bits transmitted by index $\tilde{\mathbf{B}}_{\mathrm{plim},m}(K, Q(S_m, \alpha)) \in \mathcal{B}_{\mathrm{plim},m}(K, Q(S_m, \alpha))$ as follows:

$$\tilde{\mathbf{B}}_{\mathrm{plim},m} = \mathcal{F}^{-1}\left(\tilde{k}_m, \tilde{q}_m\right). \tag{11}$$

Finally, the GW combines the two information bit sequences to recover the original data sequence as

$$\tilde{\mathbf{B}}_m = \left[(\tilde{\mathbf{B}}_{\mathrm{plim},m})^T, (\tilde{\mathbf{B}}_{\mathrm{pl},m})^T \right]^T, \tag{12}$$

where $(.)^T$ denotes transpose operation.

TABLE 1. Simulation parameters.

Parameters	Values
Simulation area, $L \times L$	1×1 [km^2]
Number of LoRaWAN nodes, M	1000
Transmission power, P_{t}	13 [dBm]
Carrier frequency, f_{c}	923 [MHz]
Bandwidth, W	125 [kHz]
Number of frequency channels, K	16
Coding rate R	4/7
Packet generation interval, $T_{\mathrm{frame},m}$	10 [min]
Duty cycle, Q_{DC}	0.01
Spreading factor, S	{7, 8, 9, 10}
Maximum payload size, $B_{\mathrm{pl}}^{\max}(S_m)$	{170, 85, 34, 5} [byte]
Overhead size, B_{oh}	15 [byte]
Number of preamble & overhead symbols, N_{p}	20.25
SNR threshold, Γ_{SNR}	{-7.5,-10,-12.5,-15} [dB]
SIR threshold, Γ_{SIR}	{-11,-13,-16,-19} [dB]
Time slot scaling factor, α	{1, 1.2, $\cdots$, 500}
Pathloss parameters (a, b, c)	(4.0, 9.5, 4.5)
Additional loss, L_{urban}	6.8 [dB]
Noise power spectral density, N_0	-174 [dBm/Hz]
Noise figure, NF	10 [dB]
Shadowing standard deviation, σ	3.48 [dB]

V. COMPUTER SIMULATION

The simulation parameters are listed in Table 1. The LoRaWAN parameters follow Japanese parameter configuration AS923 [5], i.e., $S_m \in \{7, 8, 9, 10\}$. SNR threshold $\Gamma_{\mathrm{SNR},S_m}$ and SIR threshold $\Gamma_{\mathrm{SIR},S_m}$ are depicted in Table 2. The overhead size B_{oh} is set to 15 [byte], including the MAC header (1 [byte]), message integrity code (MIC) (4 [byte]), frame header (7 [byte]), frame port (1 [byte]), and payload cyclic redundancy check (CRC) (2 [byte]) [24].

TABLE 2. Data rate and SNR limit.

Spreading factor (SF)	Data rate [bps] [2]	SNR threshold $\Gamma_{\mathrm{SNR},S_m}$ [dB] [2]	SIR threshold $\Gamma_{\mathrm{SIR},S_m}$ [dB] [11]
7	5360	-7.5	-11
8	3125	-10	-13
9	1758	-12.5	-16
10	977	-15	-19

TABLE 3. Performance comparison between the conventional LoRaWAN and LoRaWAN with PLIM. Average number of bits conveyed by a data packet (Average PDR).

SF	LoRaWAN (Periodic)	LoRaWAN (Random)	LoRaWAN with PLIM	Improvement over LoRaWAN (Random) [%]
7	1153.23 (84.7%)	1158.38 (85.1%)	1167.60 (85%)	0.80%
8	626.50 (92.1%)	627.11 (92.2%)	638.84 (92.2%)	1.87%
9	259.84 (95.5%)	260.13 (95.6%)	272.54 (95.6%)	4.77%
10	38.72 (96.8%)	38.73 (96.8%)	51.31 (96.8%)	32.5%

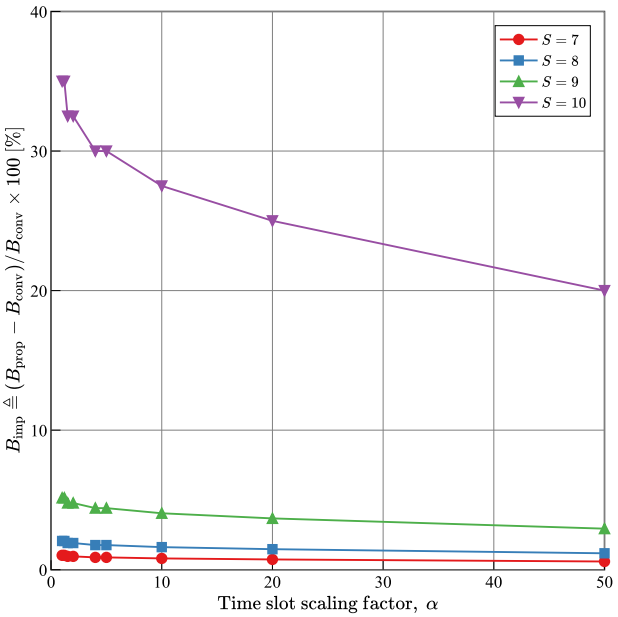

FIGURE 6. Impact of time slot scaling factor α on the performance improvement of LoRaWAN with PLIM compared to the conventional LoRaWAN.

The payload size B_{pl} is set to the maximum MAC payload size that can be transmitted by a packet for each SF at coding rate $R = 4/7$, which satisfies the dwell time limitation of 400 [ms] [5]. The total number of preamble CSS symbols and overhead CSS symbols is $N_{\mathrm{p}} = 12.25 + 8 = 20.25$. The packet generation interval is set to $T_{\mathrm{frame},m} = 10$ [min] for all the LoRaWAN nodes, except for those in Fig. 8. From (6), the number of time slots, which are used for the index, becomes $Q(S_m, \alpha) = 512$, when $T_{\mathrm{frame},m} = 10$ [min].

We assume that each LoRaWAN node sends an unconfirmed packet. Thus, there is no acknowledgment (ACK) signal from the GW and retransmission is not considered. In this study, we assume that the GW can ideally obtain the index, i.e., $(\tilde{q}_m, \tilde{k}_m) = (q_m, k_m), \forall m \in \mathcal{M}$. The obtainment of the index and the impact of incorrect estimation of the index on the performance are important future research topics.

In this study, pathloss and log-normally distributed shadowing are considered for the channel model. The received signal power of LoRaWAN node m at the GW, $P_{\mathrm{r},m}$, [dBm], is given by

$$P_{\mathrm{r},m} = P_{\mathrm{t}} - P_{\mathrm{Loss}}(d_m) + \psi(x_m, y_m), \tag{13}$$

where P_{t} [dBm] is the transmit power common to all the LoRaWAN nodes, $P_{\mathrm{Loss}}(d_m)$ [dB] is the pathloss component, where d_m is the distance between LoRaWAN node m and the GW, and $\psi(x, y_m)$ [dB] is the shadowing observed at location (x_m, y_m) of LoRaWAN node m.

The pathloss component $P_{\mathrm{Loss}}(d_m)$ is given by [25, Eq. (61)]

$$P_{\mathrm{Loss}}(d_m) = 10\, a \log_{10} d_m + b + 10\, c \log_{10} f_{\mathrm{c}} + L_{\mathrm{urban}}, \tag{14}$$

where f_{c} [MHz] is the carrier frequency. Propagation parameters a, b, and c are the coefficients for the distance, offset, and frequency loss component, respectively. L_{urban} is the additional loss due to the environment [25]. Shadowing component $\psi(x_m, y_m)$ follows the log-normal distribution, i.e., $\psi \sim \mathcal{N}(0, \sigma^2)$, where σ [dB] is the standard derivation. A spatially correlated shadowing model [26] is adopted for $\psi(x_m, y_m)$.

SNR $\gamma_{\mathrm{SNR},m}$ and SIR $\gamma_{\mathrm{SIR},m}$ of LoRaWAN node m are given by

$$\begin{cases} \gamma_{\mathrm{SNR},m} = P_{\mathrm{r},m} - (N_0 + 10 \log_{10} W + NF) \\ \gamma_{\mathrm{SIR},m} = P_{\mathrm{r},m} - \sum_{m' \in \mathcal{I}_m} P_{\mathrm{r},m'}, \end{cases} \tag{15}$$

where N_0 [dBm/Hz] is the noise power spectrum density, W [Hz] is the frequency bandwidth, NF [dB] is the noise figure, and $\mathcal{I}_m = \{m' | k_{m'} = k_m, m' \in \mathcal{M}\}$ is the set of interfering LoRaWAN nodes transmitting data packets that overlap with the packet transmitted by LoRaWAN node m, using the same frequency channel as node m. If multiple LoRaWAN nodes transmit data packets simultaneously on the same frequency channel, packet collision occurs at the GW. If there is any node $m' \in \mathcal{I}_m$ with $S_{m'} = S_m$, $\Gamma_{\mathrm{SIR},S_m}$ is set to 6 [dB]; otherwise, $\Gamma_{\mathrm{SIR},S_m}$ is set to the values in Table 2. The GW successfully receives the packet from LoRaWAN node m, if $\gamma_{\mathrm{SNR},m}$ and $\gamma_{\mathrm{SIR},m}$ are above thresholds $\Gamma_{\mathrm{SNR},S_m}$ and $\Gamma_{\mathrm{SIR},S_m}$, respectively.

The average packet delivery rate (PDR) and (average) number of bits conveyed by a packet are considered as the

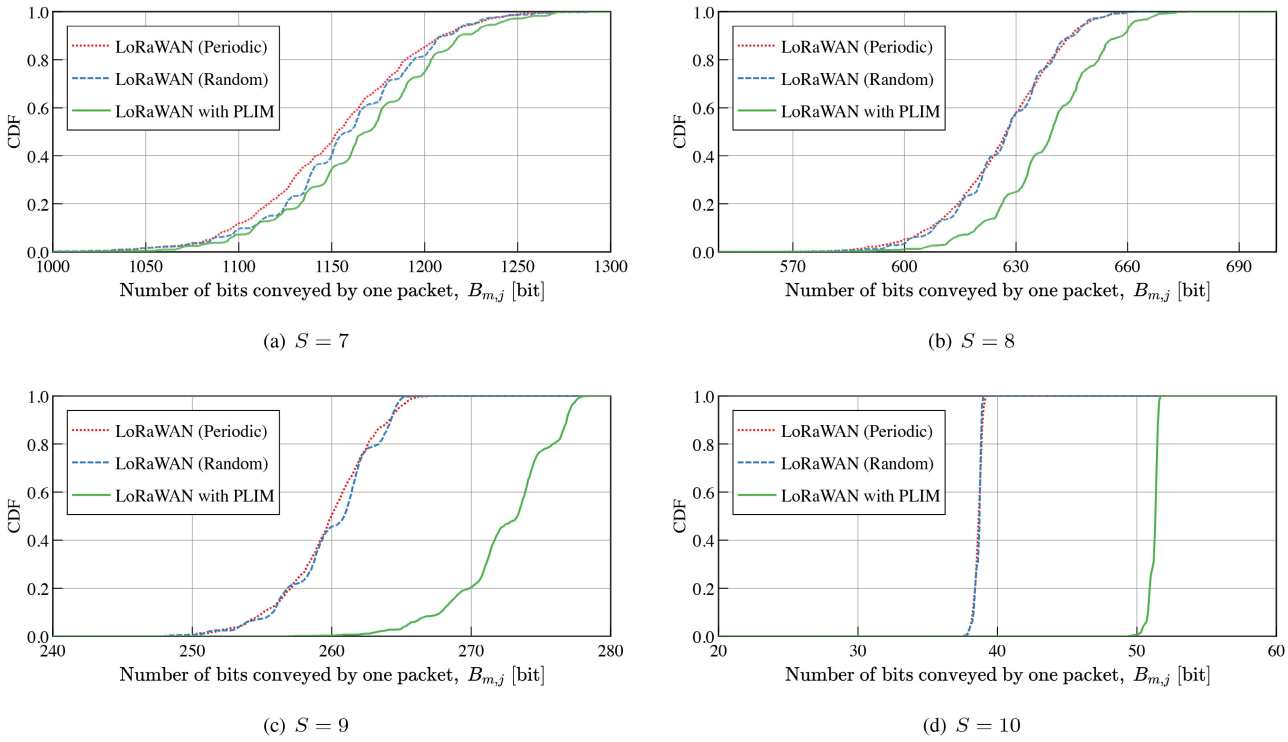

(a) $S = 7$ (b) $S = 8$

(c) $S = 9$ (d) $S = 10$

FIGURE 7. Number of bits conveyed by a LoRaWAN packet.

performance indicators. Let J be the total number of simulation runs. Let $T_{m,j}$ and $S_{m,j}$ be the total number of packets generated by LoRaWAN node $m \in \mathcal{M}$ and the number of packets successfully received by the GW during the jth simulation run, respectively. Then, the average PDR is defined as

$$P \triangleq \frac{\sum_{j=0}^{J-1} \sum_{m \in \mathcal{M}} S_{m,j}}{\sum_{j=0}^{J-1} \sum_{m \in \mathcal{M}} T_{m,j}}. \tag{16}$$

The number of bits conveyed by a packet is defined as

$$B_{m,j} \triangleq \begin{cases} B_{\mathrm{pl}} \times \left(\dfrac{S_{m,j}}{T_{m,j}}\right) \\ \qquad \text{for LoRaWAN} \\ \left(B_{\mathrm{pl}} + B_{plim,m}(K, Q(S_m, \alpha))\right) \times \left(\dfrac{S_{m,j}}{T_{m,j}}\right) \\ \qquad \text{for LoRaWAN with PLIM.} \end{cases} \tag{17}$$

The *average* number of bits conveyed by a packet is defined as

$$\overline{B} \triangleq \frac{\sum_{j=0}^{J-1} \sum_{m \in \mathcal{M}} B_{m,j}}{\sum_{j=0}^{J-1} \sum_{m \in \mathcal{M}} T_{m,j}} \tag{18}$$

For performance comparison, we consider two LoRaWAN protocols. In the first one (LoRaWAN (Periodic)), each LoRaWAN node transmits its own data packet periodically, i.e., every $T_{\mathrm{frame},m}$ [s]. In the second (LoRaWAN (Random)), LoRaWAN node m waits for a random time within $T_{\mathrm{frame},m}$ and then transmits the data packet.

A. PERFORMANCE LIMITS OF LoRaWAN WITH PLIM

The packet length becomes $T_{\mathrm{pckt},m} = \{399.6, 399.9, 398.3, 395.3\}$ [ms] for $S_m = \{7, 8, 9, 10\}$ according to $B_{\mathrm{pl}}^{\max}(S_m)$ in Table 1. As α increases, the system is more robust against timing jitter at the cost of reduction in the number of time slots. Figure 6 illustrates the impact of time slot scaling factor α on the performance improvement of LoRaWAN with PLIM compared to the conventional LoRaWAN. The performance improvement B_{imp} [%] is defined as

$$B_{\mathrm{imp}} \triangleq \left(\frac{B_{\mathrm{prop}} - B_{\mathrm{conv}}}{B_{\mathrm{conv}}}\right) \times 100, \tag{19}$$

where B_{prop} and B_{conv} are the number of bits conveyed by a packet in the conventional LoRaWAN and LoRaWAN with PLIM, given by Eq. (4) and Eq. (8), respectively. Figure 6 shows that the performance improvement of the proposed PLIM is greater, when the time slot scaling factor α is small and the spreading factor S is larger.

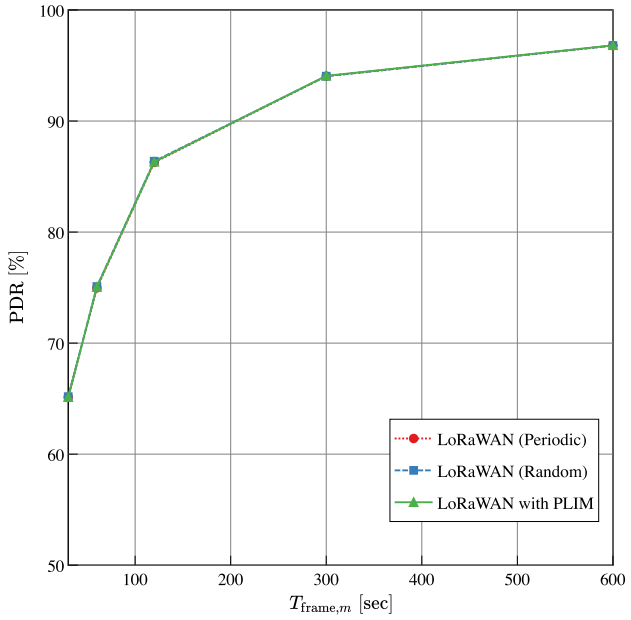

(a) PDR

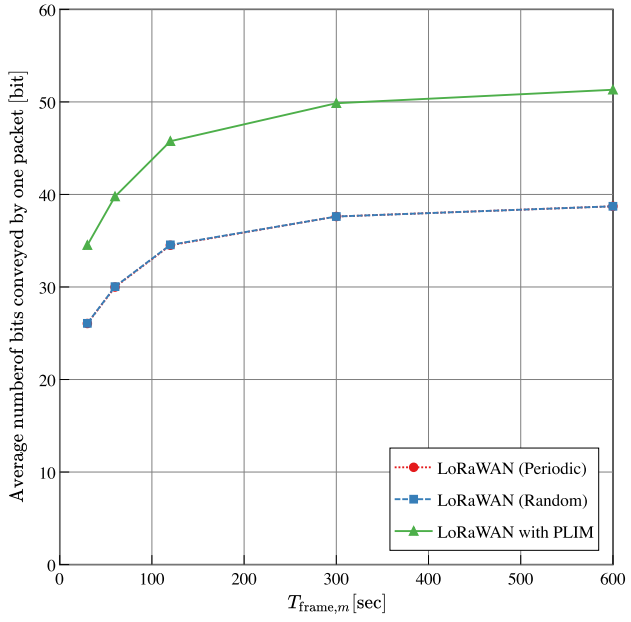

(b) Number of bits conveyed by a packet

FIGURE 8. Impact of packet generation interval $T_{\text{frame},m}$ [s].

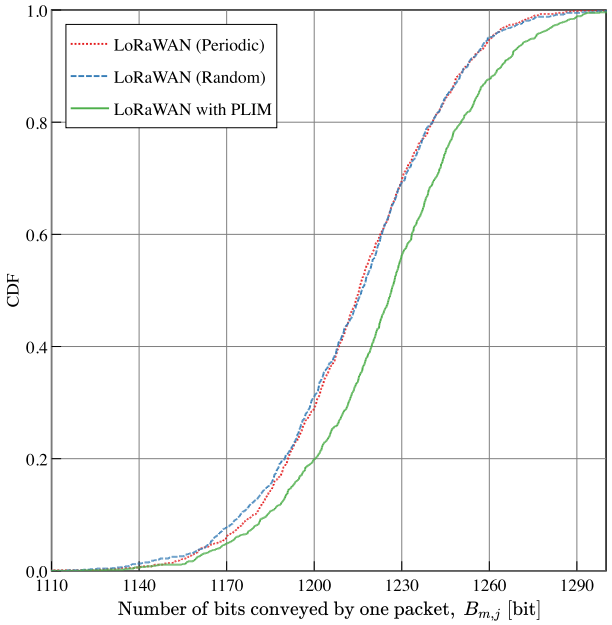

FIGURE 9. Number of bits conveyed by a LoRaWAN packet when adaptive SF allocation is adopted.

B. PERFORMANCE COMPARISON BETWEEN THE CONVENTIONAL LoRaWAN AND LoRaWAN WITH PLIM WITH A FIXED SF

Table 3 summarizes the performance comparison between the conventional LoRaWAN and LoRaWAN with PLIM; the proposed PLIM increases the average number of bits conveyed by a LoRaWAN data packet, e.g., up to 32.5% with $S_m = 10$.

This performance improvement becomes more significant as the SF increases, which can be explained as follows. As shown in Table 1, the maximum payload size $B_{\text{pl}}^{\max}(S_m)$ in a packet decreases as SF increases, whereas the packet length T_{pckt} is almost constant. This indicates that the number of available time slots $Q(S_m, \alpha)$ is also almost constant. Thus, the number of bits conveyed by the index relative to the number of bits within a data packet increases. Fig. 7 depicts the cumulative distribution function (CDF) of the number of bits conveyed by a LoRaWAN packet when different SF S are used. Each LoRaWAN node periodically transmits in LoRaWAN (Periodic). Thus, if there is another LoRaWAN node whose transmission timing is the same as those of the other LoRaWAN nodes, the transmitted packets always collide with each other. The distribution of the number of bits conveyed by a packet for LoRaWAN (Periodic) is considerably greater than that of LoRaWAN (Random). Thus, we can conclude that the proposed PLIM is more effective when the wireless channel environment is harsh, where each LoRaWAN node needs to use larger SF.

Fig. 8 displays the impact of the packet generation interval $T_{\text{frame},m}$ [s] on the average PDR performance and average number of bits conveyed by a packet $\overline{B}$. The SF is set to $S_m = 10$. Fig. 8 (a) shows that the average PDR performance improves as $T_{\text{frame},m}$ increases due to the reduction in the packet collision probability. When $T_{\text{frame},m}$ is short, the number of time slots $Q(S_m, \alpha)$ reduces. Thus, the achievable gain by the proposed PLIM becomes less significant. However, it still shows significant performance improvement over LoRaWAN (Periodic) and LoRaWAN (Random).

C. PERFORMANCE COMPARISON BETWEEN LoRaWAN AND LoRaWAN WITH PLIM WITH A VARIABLE SF

Figure 9 shows the CDF of the number of bits conveyed by a LoRaWAN packet when variable SF allocation is considered. LoRaWAN node m selects the least SF, whose SNR threshold

$\Gamma_{\mathrm{SNR},S_m}$ (Table 2) is lower than SNR $\gamma_{\mathrm{SNR},m}$ (Eq. (15)). As observed in the figure, the proposed PLIM can increase the number of bits conveyed by a packet compared to the conventional LoRaWAN (Periodic) and LoRaWAN (Random), even with variable SF allocation.

VI. CONCLUSION

This study proposed *packet-level index modulation (PLIM)* for LoRaWAN, which takes advantage of the sparse data packet transmission in time of each LoRaWAN node. The periodic transmission interval is split into several time slots, which are not necessarily synchronized among the LoRaWAN nodes in the system. When a LoRaWAN node transmits a packet, the node selects one of the time slots and frequency channels to indicate the data. Computer simulation results demonstrated that the proposed PLIM can increase the transmission data rate compared to the conventional LoRaWAN. When each LoRaWAN node transmits a packet every 10 [min] with an SF of 10, the proposed PLIM can increase the number of data bits conveyed by a data packet up to 32.5%, compared to the conventional LoRaWAN.

The proposed PLIM has several advantages: Modifications in the current LoRaWAN standardization are not required, and stringent synchronization is not required among the LoRaWAN nodes.

The actual implementation of the proposed PLIM is intended in the future. In this manuscript, we have assumed ideal synchronization between each LoRaWAN node and the GW. However, it is known that LoRaWAN nodes exhibit clock drift due to their simple structure. Since the clock drift may degrade the detection accuracy of the time index, the evaluation of the proposed PLIM's performance in the presence of such clock drift is left as an important future study. Furthermore, how to compensate for the negative effect of clock drift is also one of the interesting research directions.

REFERENCES

[1] L. Vangelista, "Frequency shift chirp modulation: The LoRa modulation," *IEEE Signal Process. Lett.*, vol. 24, no. 12, pp. 1818–1821, Dec. 2017.
[2] A. Waret, M. Kaneko, A. Guitton, and N. El Rachkidy, "LoRa throughput analysis with imperfect spreading factor orthogonality," *IEEE Wireless Commun. Lett.*, vol. 8, no. 2, pp. 408–411, Apr. 2019.
[3] C. Goursaud and J.-M. Gorce, "Dedicated networks for IoT: PHY/MAC state of the art and challenges," *EAI Endorsed Trans. Internet Things*, vol. 1, no. 1, pp. 1–11, Oct. 2015. [Online]. Available: https://hal.archives-ouvertes.fr/hal-01231221
[4] F. Adelantado, X. Vilajosana, P. Tuset-Peiro, B. Martinez, J. Melia-Segui, and T. Watteyne, "Understanding the limits of LoRaWAN," *IEEE Commun. Mag.*, vol. 55, no. 9, pp. 34–40, Sep. 2017.
[5] LoRa Alliance Technical Committee. (2018). *LoRaWAN Regional Parameters v1.1 REV A*. [Online]. Available: https://lora-alliance.org/resource-hub/lorawanr-regional-parameters-v11ra
[6] M. El-Aasser, T. Elshabrawy, and M. Ashour, "Joint spreading factor and coding rate assignment in LoRaWAN networks," in *Proc. IEEE Global Conf. Internet Things (GCIoT)*, Dec. 2018, pp. 1–7.
[7] J.-T. Lim and Y. Han, "Spreading factor allocation for massive connectivity in LoRa systems," *IEEE Commun. Lett.*, vol. 22, no. 4, pp. 800–803, Apr. 2018.
[8] D. Garlisi, I. Tinnirello, G. Bianchi, and F. Cuomo, "Capture aware sequential waterfilling for LoRaWAN adaptive data rate," *IEEE Trans. Wireless Commun.*, early access, Dec. 1, 2020, doi: 10.1109/TWC.2020.3038638.
[9] J. Ortin, M. Cesana, and A. Redondi, "How do ALOHA and listen before talk coexist in LoRaWAN?" in *Proc. IEEE 29th Annu. Int. Symp. Pers., Indoor Mobile Radio Commun. (PIMRC)*, Bologna, Italy, Sep. 2018, pp. 1–7.
[10] J. Ortin, M. Cesana, and A. Redondi, "Augmenting LoRaWAN performance with listen before talk," *IEEE Trans. Wireless Commun.*, vol. 18, no. 6, pp. 3113–3128, Jun. 2019.
[11] N. Aihara, K. Adachi, O. Takyu, M. Ohta, and T. Fujii, "Q-learning aided resource allocation and environment recognition in LoRaWAN with CSMA/CA," *IEEE Access*, vol. 7, pp. 152126–152137, Dec. 2019.
[12] M. Omer Farooq, "Introducing scalability in LoRa-based networks through multi-hop communication setups," in *Proc. IEEE Global Commun. Conf. (GLOBECOM)*, Waikoloa, HI, USA, Dec. 2019, pp. 1–6.
[13] J. Haxhibeqiri, I. Moerman, and J. Hoebeke, "Low overhead scheduling of LoRa transmissions for improved scalability," *IEEE Internet Things J.*, vol. 6, no. 2, pp. 3097–3109, Apr. 2019, doi: 10.1109/JIOT.2018.2878942.
[14] T. Elshabrawy and J. Robert, "Interleaved chirp spreading LoRa-based modulation," *IEEE Internet Things J.*, vol. 6, no. 2, pp. 3855–3863, Apr. 2019.
[15] M. Di Renzo, H. Haas, A. Ghrayeb, S. Sugiura, and L. Hanzo, "Spatial modulation for generalized MIMO: Challenges, opportunities, and implementation," *Proc. IEEE*, vol. 102, no. 1, pp. 56–103, Jan. 2014.
[16] N. Ishikawa, S. Sugiura, and L. Hanzo, "Subcarrier-index modulation aided OFDM—Will it work?" *IEEE Access*, vol. 4, pp. 2580–2593, 2016.
[17] S. Althunibat, R. Mesleh, and T. Faizur Rahman, "A novel uplink multiple access technique based on index-modulation concept," *IEEE Trans. Commun.*, vol. 67, no. 7, pp. 4848–4855, Jul. 2019.
[18] S. Sugiura, T. Ishihara, and M. Nakao, "State-of-the-art design of index modulation in the space, time, and frequency domains: Benefits and fundamental limitations," *IEEE Access*, vol. 5, pp. 21774–21790, 2017.
[19] S. Althunibat, R. Mesleh, and K. A. Qaraqe, "IM-OFDMA: A novel spectral efficient uplink multiple access based on index modulation," *IEEE Trans. Veh. Technol.*, vol. 68, no. 10, pp. 10315–10319, Oct. 2019.
[20] M. Chafii, F. Bader, and J. Palicot, "SC-FDMA with index modulation for M2M and IoT uplink applications," in *Proc. IEEE Wireless Commun. Netw. Conf. (WCNC)*, Apr. 2018, pp. 1–6.
[21] M. Au, G. Kaddoum, M. S. Alam, E. Basar, and F. Gagnon, "Joint code-frequency index modulation for IoT and multi-user communications," *IEEE J. Sel. Topics Signal Process.*, vol. 13, no. 6, pp. 1223–1236, Oct. 2019.
[22] M. Nakao, T. Ishihara, and S. Sugiura, "Single-carrier frequency-domain equalization with index modulation," *IEEE Commun. Lett.*, vol. 21, no. 2, pp. 298–301, Feb. 2017.
[23] J. Haxhibeqiri, I. Moerman, and J. Hoebeke, "Low overhead scheduling of LoRa transmissions for improved scalability," *IEEE Internet Things J.*, vol. 6, no. 2, pp. 3097–3109, Apr. 2019.
[24] J. Haxhibeqiri, E. De Poorter, I. Moerman, and J. Hoebeke, "A survey of LoRaWAN for IoT: From technology to application," *Sensors*, vol. 18, no. 11, pp. 1–38, Nov. 2018.
[25] P Series. (2015). *Propagation Data and Prediction Methods for the Planning of Short-Range Outdoor Radiocommunication Systems and Radio Local Area Networks in the Frequency Range 300 MHz to 100 GHz*. [Online]. Available: https://www.itu.int/rec/R-REC-P.1411/en
[26] H. Claussen, "Efficient modelling of channel maps with correlated shadow fading in mobile radio systems," in *Proc. IEEE 16th Int. Symp. Pers., Indoor Mobile Radio Commun.*, Sep. 2005, pp. 512–516.

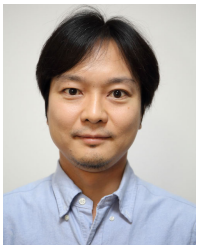

KOICHI ADACHI (Senior Member, IEEE) received the B.E., M.E., and Ph.D. degrees in engineering from Keio University, Japan, in 2005, 2007, and 2009 respectively. His research interests include cooperative communications and energy efficient communication technologies.

From 2007 to 2010, he was a Research Fellow with the Japan Society for the Promotion of Science. He was a Visiting Researcher with the City University of Hong Kong in 2009 and a Visiting Research Fellow with the University of Kent in 2009. From 2010 to 2016, he was with the Institute for Infocomm Research, A*STAR, Singapore.

He is currently an Associate Professor with The University of Electro-Communications, Japan. He is a member of the IEICE. He served as the General Co-Chair for the 10th and 11th IEEE Vehicular Technology Society Asia–Pacific Wireless Communications Symposium, the Track Co-Chair for transmission technologies and communication theory of the 78th and 80th IEEE Vehicular Technology Conference in 2013 and 2014, respectively, the symposium Co-Chair for the communication theory symposium of the IEEE Globecom 2018, the Tutorial Co-Chair of the IEEE ICC 2019, and the Symposium Co-Chair for the wireless communications symposium of the IEEE Globecom 2020. He was an Associate Editor of the *IET Transactions on Communications* from 2015 to 2017, IEEE TRANSACTIONS ON VEHICULAR TECHNOLOGY form 2016 to 2018, and the IEEE OPEN JOURNAL OF VEHICULAR TECHNOLOGY since 2019. He has been an Associate Editor of the IEEE WIRELESS COMMUNICATIONS LETTERS since 2016 and the IEEE TRANSACTIONS ON GREEN COMMUNICATIONS AND NETWORKING since 2016.

Dr. Adachi was recognized as the Exemplary Reviewer of the IEEE WIRELESS COMMUNICATIONS LETTERS from 2012 to 2015. He was a recipient of the Excellent Editor Award from the IEEE ComSoc MMTC in 2013. He was a co-recipient of the WPMC2020 Best Student Paper Award.

KOHEI TSURUMI is currently pursuing the B.E. degree with The University of Electro-Communications. His research interests include LPWA networks.

AOTO KABURAKI (Graduate Student Member, IEEE) received the B.E. degree in information and communication engineering from The University of Electro-Communications in 2020, where he is currently pursuing the M.E. degree. His research interests include machine learning and its application to wireless communication.

OSAMU TAKYU (Member, IEEE) received the B.E. degree in electrical engineering from the Tokyo University of Information Sciences, Chiba, Japan, in 2002, and the M.E. and Ph.D. degrees in open and environmental systems from Keio University, Yokohama, Japan, in 2003 and 2006, respectively. His current research interests include wireless communication systems and distributed wireless communication technology.

From 2003 to 2007, he was a Research Associate with the Department of Information and Computer Science, Keio University. From 2004 to 2005, he was a Visiting Scholar with the School of Electrical and Information Engineering, University of Sydney. From 2007 to 2011, he was an Assistant Professor with the Department of Electrical Engineering, Tokyo University of Science. From 2011 to 2013, he was an Assistant Professor with the Department of Electrical and Computer Engineering, Shinshu University, where he has been an Associate Professor, since 2013.

Dr. Takyu was a recipient of the Young Researcher's Award of the IEICE 2010, the 2010 Active Research Award in radio communication systems (RCS) from the IEICE Technical Committee on RCS, and the 2018 Best Paper Award in smart radio (SR) from IEICE Technical Committee on SR.

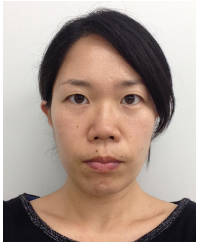

MAI OHTA (Member, IEEE) received the B.E., M.E., and Ph.D. degrees in electrical engineering from The University of Electro-Communications, Tokyo, Japan, in 2008, 2010, and 2013, respectively. Her research interests include cognitive radio, spectrum sensing, LPWAN, and sensor networks.

Since 2013, she has been an Assistant Professor with the Department of Electronics Engineering and Computer Science, Fukuoka University.

Dr. Ohta was a recipient of the Young Researcher's Award from the IEICE in 2013.

TAKEO FUJII (Member, IEEE) received the B.E., M.E., and Ph.D. degrees in electrical engineering from Keio University, Yokohama, Japan, in 1997, 1999, and 2002, respectively. His current research interests include cognitive radio and ad-hoc wireless networks.

From 2000 to 2002, he was a Research Associate with the Department of Information and Computer Science, Keio University. From 2002 to 2006, he was an Assistant Professor with the Department of Electrical and Electronic Engineering, Tokyo University of Agriculture and Technology. From 2006 to 2014, he was an Associate Professor with the Advanced Wireless Communication Research Center, The University of Electro-Communications, where he is currently a Professor and the Director He is a Fellow of the IEICE.

Dr. Fujii received the Best Paper Award from the IEEE VTC 1999, the 2001 Active Research Award in radio communication systems (RCS) from the IEICE technical Committee of RCS, the 2001 Ericsson Young Scientist Award, the Young Researcher's Award from the IEICE in 2004, The Young Researcher Study Encouragement Award from the IEICE Technical Committee of AN in 2009, the Best Paper Award from the IEEE CCNC 2013, and the IEICE Communication Society Best Paper Award in 2016.